Elucidation of the Na2/3FePO4 and Li2/3FePO4 intermediate superstructure revealing a pseudouniform ordering in 2D

Florent Boucher,* Joël Gaubicher, Marine Cuisinier, Dominique Guyomard and Philippe Moreau

Institut des Matériaux Jean Rouxel (IMN), Univesité de Nantes-CNRS, UMR6502, 2 rue de la Houssinière, BP 32229, 44322 Nantes Cedex, France

Correspondence email: Florent.Boucher@cnrs-imn.fr

Synthesis and crystallization

The $Na_{2/3}FePO_4$ intermediate composition was electrochemically synthesized, as previously described, by using a positive electrode made with a mixture of 70% $FePO_4$ (olivine) and 30% carbon black (Ketjen). $FePO_4$ was obtained from $LiFePO_4$ by chemical oxidation in acetonitrile, using NO_2BF_6 (Aldrich). The mixture was then ball-milled (30 min, 500 rpm) and pasted onto an Al current collector. Electrodes and powders were kept in a dry argon glove box to avoid any side reactions of the FePO4 with air. SwagelokTM-type batteries were mounted with sodium as the negative and reference electrode, and 1M $NaClO_4$ in PC as the electrolyte. Batteries were cycled in potentiodynamic mode (PITT, VMP-Biologic SA, Claix, France), with step duration being restricted by a current limit. The latter was set to be equivalent to nominal 1 Na/200 h. The $Na_{2/3}FePO_4$ phase was obtained with high precision (x=0.66) during the charge of the battery by equilibrating the sample at 2.95V versus Na/Na^+.

Refinement

Rietveld analyses were achieved by using the FullProf Suite software. Since the superstructure corresponding to the Na/vacancy ordering only generates a few additional diffraction peaks, a few constraints had to be applied to the structural refinement in order to avoid divergences and inconsistencies. Similarity was imposed with respect to isotropic displacement parameters for a given atomic species, and they were furthermore fixed in the case of oxygen atoms (B_{iso}=0.25 $Å^2$). Additionally, soft constraints were used on the P—O bond lengths (1.53 (1) Å). In this manner, correlation coefficients were maintained below 87 % and all of the atomic coordinates were able to be refined. Angular-dependent shapes of the diffracted intensities were fitted using a Thompson-Cox-Hastings pseudo-Voigt function. Selective size-broadening parameters were used for the supercell reflections ($h = 3n \pm 1$ & $h = 3n \pm 2$) in order to accommodate the smaller coherence length associated with the Na/vacancy ordering.

Computing details

Data collection: MAR345 image plate integration; cell refinement: FULLPROF; data reduction: FULLPROF; program(s) used to refine structure: FULLPROF.

(Na2/3FePO4)

Crystal data

Na2/3$FePO_4$
M_r = 498.44
Monoclinic, $P2_1/n$
Hall symbol: -P 2yn
a = 18.23736 (14) Å
b = 4.93687 (4) Å
c = 11.96092 (11) Å
β = 120.7221 (7)°
V = 925.77 (1) $Å^3$

Z = 4
F(000) = 964
D_x = 3.576 Mg m^{-3}
Synchrotron radiation, λ = 0.725633 Å
μ = 5.60 mm^{-1}
T = 293 K
Particle morphology: nanometric particles
black
?, 10 × 0.5 mm

Data collection

2-circle diffractometer
Radiation source: synchrotron
Si(111) monochromator

Specimen mounting: sealed capillarry
Data collection mode: transmission
Scan method: step
$2\theta_{min}$ = 0.04°, $2\theta_{max}$ = 35.01°, $2\theta_{step}$ = 0.01°

Refinement

R_p = 0.757
R_{wp} = 1.097
R_{exp} = 1.411
R_{Bragg} = 1.353
χ^2 = 0.604
3498 data points
Excluded region(s): below 4.7 and from 33.7 to 35.0

Profile function: Thompson-Cox-Hastings pseudo-Voigt
103 parameters
12 restraints
5 constraints
$(\Delta/\sigma)_{max}$ = 0.05
Background function: Linearly interpolated

Fractional atomic coordinates and isotropic or equivalent isotropic displacement parameters (Å²)

	x	y	z	U_{iso}*/U_{eq}
Fe1	0.1503 (4)	0.9687 (16)	0.2151 (6)	0.0056 (5)*
Fe2	0.5077 (4)	0.013 (2)	0.7864 (7)	0.0056 (5)*
Fe3	0.8247 (5)	1.0014 (12)	0.2186 (7)	0.0056 (5)*
Na1	0.6598 (7)	0.974 (3)	0.5219 (10)	0.012 (2)*
Na2	0.8427 (10)	0.012 (4)	0.5032 (16)	0.012 (2)*
P1	0.2146 (6)	0.4518 (16)	0.3945 (8)	0.0046 (7)*
P2	0.4523 (5)	0.5683 (16)	0.6113 (7)	0.0046 (7)*
P3	0.8829 (5)	0.4377 (17)	0.3968 (8)	0.0046 (7)*
O1	0.2185 (14)	0.751 (2)	0.372 (3)	0.00317*
O2	0.462 (2)	0.260 (2)	0.624 (3)	0.00317*
O3	0.8755 (18)	0.747 (2)	0.393 (2)	0.00317*
O4	0.0962 (17)	0.131 (4)	0.0360 (11)	0.00317*
O5	0.5715 (16)	0.829 (4)	0.9611 (13)	0.00317*
O6	0.7664 (16)	0.144 (6)	0.0377 (13)	0.00317*
O7	0.1249 (10)	0.311 (5)	0.327 (3)	0.00317*
O8	0.7537 (16)	0.698 (4)	0.687 (2)	0.00317*
O9	0.7883 (8)	0.334 (4)	0.328 (2)	0.00317*
O10	0.4083 (19)	0.702 (5)	0.678 (3)	0.00317*
O11	0.4617 (9)	0.287 (4)	0.322 (3)	0.00317*
O12	0.0710 (17)	0.695 (5)	0.667 (3)	0.00317*

Geometric parameters (Å, º) for (Na2/3FePO4)

Na1—O4^{i}	2.32 (3)	P3—O3	1.532 (13)
Na1—O8	2.29 (2)	P3—O9	1.570 (16)
Na1—O1^{ii}	2.35 (2)	P3—O5^{v}	1.557 (17)
Na1—O6^{iii}	2.44 (3)	Fe1—O11^{x}	2.06 (2)
Na1—O10^{ii}	2.61 (3)	Fe1—O7^{xi}	2.34 (3)
Na1—O2^{iv}	2.31 (3)	Fe1—O1	1.96 (3)
Na2—O5^{v}	2.10 (3)	Fe1—O8^{ii}	2.25 (2)
Na2—O3^{vi}	2.15 (4)	Fe1—O8^{xii}	2.24 (3)
Na2—O9	2.40 (3)	Fe1—O4^{xi}	2.011 (15)
Na2—O6^{vii}	2.55 (4)	Fe2—O12^{xiii}	2.00 (4)
Na2—O1^{iv}	2.56 (4)	Fe2—O5^{vi}	2.015 (17)
Na2—O7^{viii}	2.41 (4)	Fe2—O7^{xiv}	2.12 (2)
P1—O6^{ix}	1.548 (17)	Fe2—O11^{viii}	2.22 (3)
P1—O7	1.57 (2)	Fe2—O2	2.07 (3)
P1—O1	1.510 (15)	Fe2—O10^{vi}	2.22 (3)
P1—O8^{iv}	1.55 (3)	Fe3—O10^{xv}	2.08 (4)
P2—O10	1.54 (4)	Fe3—O6^{xi}	1.989 (18)
P2—O2	1.531 (13)	Fe3—O9^{iii}	2.017 (18)
P2—O11^{iv}	1.526 (17)	Fe3—O9^{xi}	2.40 (2)
P2—O4^{x}	1.546 (14)	Fe3—O3	2.19 (2)
P3—O12^{iv}	1.54 (4)	Fe3—O12^{ii}	2.25 (3)
O1^{ii}—Na1—O10^{ii}	91.0 (9)	O5^{v}—P3—O9	106.9 (11)
O1^{ii}—Na1—O2^{iv}	167.3 (8)	O7^{xi}—Fe1—O11^{x}	88.5 (9)
O1^{ii}—Na1—O4^{i}	81.0 (7)	O1—Fe1—O11^{x}	92.4 (10)
O1^{ii}—Na1—O8	78.1 (9)	O8^{ii}—Fe1—O11^{x}	148.6 (10)
O1^{ii}—Na1—O6^{iii}	91.9 (8)	O8^{xii}—Fe1—O11^{x}	128.8 (11)
O4^{i}—Na1—O8	128.3 (9)	O4^{xi}—Fe1—O11^{x}	92.9 (11)
O4^{i}—Na1—O6^{iii}	162.5 (11)	O1—Fe1—O7^{xi}	93.6 (8)
O2^{iv}—Na1—O4^{i}	98.7 (7)	O7^{xi}—Fe1—O8^{ii}	60.2 (8)
O4^{i}—Na1—O10^{ii}	61.9 (7)	O7^{xi}—Fe1—O8^{xii}	141.2 (10)
O2^{iv}—Na1—O10^{ii}	77.9 (9)	O4^{xi}—Fe1—O7^{xi}	100.9 (9)
O6^{iii}—Na1—O10^{ii}	102.6 (9)	O1—Fe1—O8^{ii}	87.6 (7)
O8—Na1—O10^{ii}	162.5 (10)	O1—Fe1—O8^{xii}	76.7 (8)
O2^{iv}—Na1—O6^{iii}	84.6 (7)	O1—Fe1—O4^{xi}	164.7 (7)
O2^{iv}—Na1—O8	111.1 (9)	O8^{ii}—Fe1—O8^{xii}	81.7 (10)
O3^{vi}—Na2—O5^{v}	99.6 (10)	O4^{xi}—Fe1—O8^{ii}	95.2 (8)
O3^{vi}—Na2—O7^{viii}	95.1 (10)	O4^{xi}—Fe1—O8^{xii}	88.8 (10)
O1^{iv}—Na2—O3^{vi}	168.0 (11)	O5^{vi}—Fe2—O12^{xiii}	91.7 (12)

O3^{vi}—Na2—O6^{vii}	83.3 (9)	O7^{xiv}—Fe2—O12^{xiii}	122.4 (13)
O3^{vi}—Na2—O9	89.3 (9)	O11^{viii}—Fe2—O12^{xiii}	153.3 (11)
O5^{v}—Na2—O9	67.5 (8)	O2—Fe2—O12^{xiii}	89.7 (10)
O5^{v}—Na2—O7^{viii}	119.1 (12)	O10^{vi}—Fe2—O12^{xiii}	89.2 (12)
O1^{iv}—Na2—O5^{v}	92.4 (10)	O5^{vi}—Fe2—O7^{xiv}	88.1 (11)
O5^{v}—Na2—O6^{vii}	176.9 (13)	O5^{vi}—Fe2—O11^{viii}	96.9 (9)
O1^{iv}—Na2—O7^{viii}	78.6 (10)	O2—Fe2—O5^{vi}	168.3 (8)
O6^{vii}—Na2—O7^{viii}	61.4 (9)	O5^{vi}—Fe2—O10^{vi}	99.2 (10)
O7^{viii}—Na2—O9	171.1 (12)	O7^{xiv}—Fe2—O11^{viii}	83.3 (10)
O1^{iv}—Na2—O6^{vii}	84.7 (8)	O2—Fe2—O7^{xiv}	81.3 (10)
O1^{iv}—Na2—O9	95.6 (8)	O7^{xiv}—Fe2—O10^{vi}	147.6 (12)
O6^{vii}—Na2—O9	111.7 (10)	O2—Fe2—O11^{viii}	86.9 (9)
O1—P1—O8^{iv}	106.7 (10)	O10^{vi}—Fe2—O11^{viii}	64.6 (9)
O6^{ix}—P1—O8^{iv}	109.7 (11)	O2—Fe2—O10^{vi}	92.4 (9)
O7—P1—O8^{iv}	95.2 (15)	O6^{xi}—Fe3—O10^{xv}	88.0 (12)
O1—P1—O7	118.3 (12)	O9^{iii}—Fe3—O10^{xv}	120.3 (13)
O1—P1—O6^{ix}	116.0 (11)	O9^{xi}—Fe3—O10^{xv}	154.1 (10)
O6^{ix}—P1—O7	108.7 (14)	O3—Fe3—O10^{xv}	86.7 (10)
O2—P2—O10	116.1 (12)	O10^{xv}—Fe3—O12^{ii}	88.3 (12)
O4^{x}—P2—O10	111.0 (14)	O6^{xi}—Fe3—O9^{iii}	86.7 (10)
O10—P2—O11^{iv}	101.4 (17)	O6^{xi}—Fe3—O9^{xi}	102.0 (8)
O2—P2—O4^{x}	106.4 (11)	O3—Fe3—O6^{xi}	165.5 (7)
O2—P2—O11^{iv}	112.2 (10)	O6^{xi}—Fe3—O12^{ii}	104.0 (10)
O4^{x}—P2—O11^{iv}	109.8 (14)	O9^{iii}—Fe3—O9^{xi}	84.4 (8)
O3—P3—O12^{iv}	118.1 (12)	O3—Fe3—O9^{iii}	84.5 (8)
O9—P3—O12^{iv}	109.5 (16)	O9^{iii}—Fe3—O12^{ii}	150.1 (10)
O5^{v}—P3—O12^{iv}	105.8 (14)	O3—Fe3—O9^{xi}	88.5 (6)
O3—P3—O5^{v}	111.5 (10)	O9^{xi}—Fe3—O12^{ii}	66.2 (9)
O3—P3—O9	104.7 (11)	O3—Fe3—O12^{ii}	89.3 (8)

Symmetry codes: (i) x+1/2, −y+3/2, z+1/2; (ii) −x+1, −y+2, −z+1; (iii) −x+3/2, y+1/2, −z+1/2; (iv) −x+1, −y+1, −z+1; (v) −x+3/2, y−1/2, −z+3/2; (vi) x, y−1, z; (vii) −x+3/2, y−1/2, −z+1/2; (viii) −x+1, −y, −z+1; (ix) x−1/2, −y+1/2, z+1/2; (x) −x+1/2, y+1/2, −z+1/2; (xi) x, y+1, z; (xii) x−1/2, −y+3/2, z−1/2; (xiii) −x+1/2, y−1/2, −z+3/2; (xiv) x+1/2, −y+1/2, z+1/2; (xv) x+1/2, −y+3/2, z−1/2.

Temperature-dependant *in situ* X-Ray synchrotron diffraction

Experiments were performed at SOLEIL, the French third-generation synchrotron radiation source on the CRISTAL beamline. A monochromatic beam with $\lambda = 0.725633$ Å was used and shone onto a sealed capillary (Ø 0.5 mm), inside which the powder was placed. The diffracted intensities were measured in transmission geometry ($4.7 \leq 2\theta \leq 33.7$) using a Mar image plate detector, allowing for an optimal signal to noise ratio. A LaB_6 powder sample was used for calibrating the Mar detector and determining the peak shape resolution of the apparatus. For temperature-dependent experiments, the capillary was heated up every 25°C using a calibrated high-temperature gas streamer.

The monoclinic $P2_1/n$ supercell of $Na_{2/3}FePO_4$ is maintained up to 250°C. The evolution of cell parameters as the function of the temperature is shown in **Figure 1.** Polynomial adjustment functions are given below (T in °C).

$$\mathbf{a} = 18.2310 + 3\times10^{-4}.T + 7\times10^{-7}.T^2$$
$$\mathbf{b} = 4.9353 + 8\times10^{-5}.T + 2\times10^{-7}.T^2$$
$$\mathbf{c} = 11.9590 + 8\times10^{-5}.T + 4\times10^{-8}.T^2$$
$$\boldsymbol{\beta} = 120.71 + 4\times10^{-4}.T + 2\times10^{-6}.T^2$$
$$\mathbf{V} = 925.07 + 3.36\times10^{-2}.T + 6\times10^{-5}.T^2$$

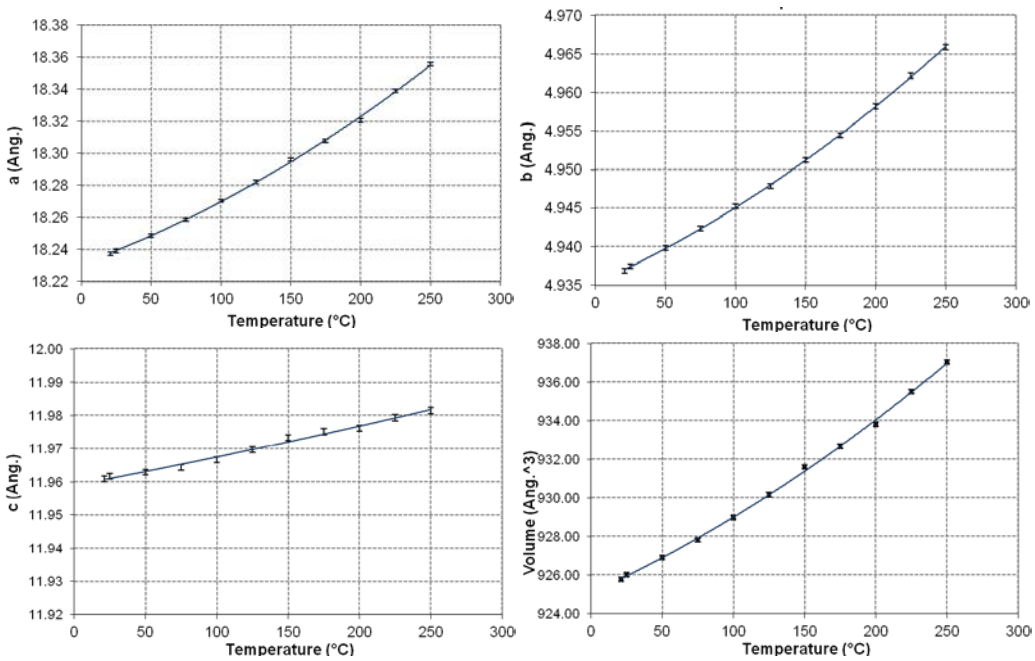

Figure 1: Evolution of the unit cell parameters and volume for $Na_{2/3}FePO_4$ as a function of temperature. Error bars represent three times the estimated standard deviation.

In Figure 2 is shown the evolution of the diffracted intensity of one superstructure peak (-2 0 2) as a function of the sample temperature. The sample was heated up from 25°C to 300°C and then cooled down to 50°C. At first, no significant evolution of the intensity is observed. The structural reorganization starts to appear above 100°C and leads to a continuous increase of the diffracted intensity till 250°C. A better coherence between the channels is established leading to an improvement of the crystallinity. Above 250°C, due to the complete delocalization of sodium atoms, the monoclinic supercell disappears and transforms into the classical orthorhombic Pnma unit cell. Back to lower temperature, the monoclinic super cell is recovered with even a stronger intensity of the (-2 0 2) peak. The sample crystallinity is clearly improved by the heat treatment at 300°C.

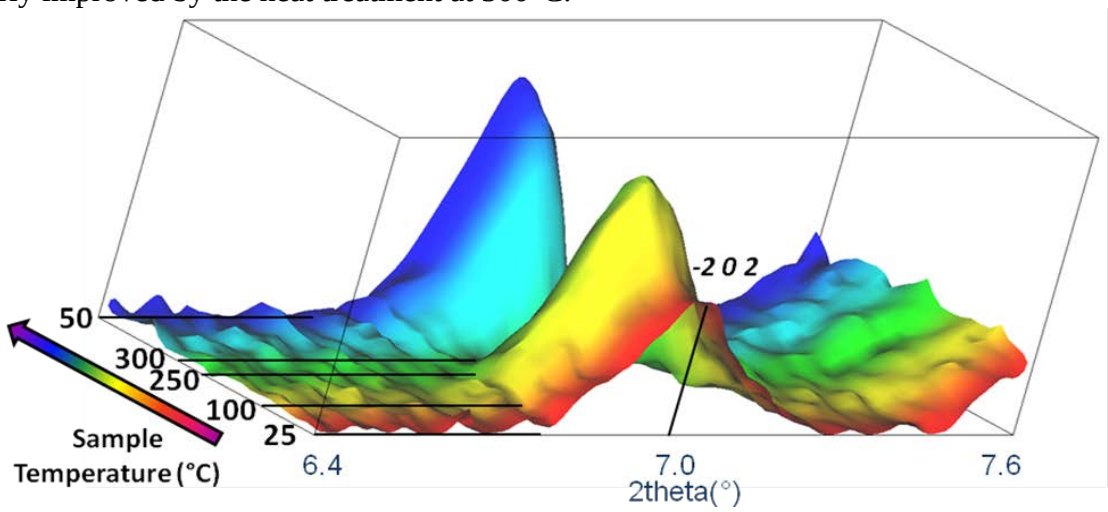

Figure 2: Evolution of the (-2 0 2) superstructure peak as a function of the sample temperature.

Geometry optimization for the olivine $Na_{2/3}FePO_4$

The electronic structure of the olivine $Na_{2/3}FePO_4$ was calculated with the VASP package[1] within the PBE[2] generalized gradient approximation (GGA). A GGA+U with (U_{eff}=4.3eV)[3] and a ferromagnetic order to better describe the correlation on the Fe d orbitals. Cell parameters were taken from experimental values while the atomic positions were optimized to minimize forces.

Details of the calculations:
Spin polarized calculation with a ferromagnetic coupling between Fe atoms
Energy Cut-Off for plane waves: 600eV
16 irreducible K-points for SCF (2, 8, 4) grid

Optimized structure of $Na_{2/3}FePO_4$:

Phase data	
Space-group	P 1 21/n 1 (14) - monoclinic
Cell	a=18.2370 Å b=4.9370 Å c=11.9609 Å β=120.7250° V=925.75 Å^3

Atomic parameters				
Atom	**Wyck.**	**x/a**	**y/b**	**z/c**
Fe1	4e	0.15620	0.98930	0.21780
Fe2	4e	0.50990	0.00640	0.78370
Fe3	4e	0.82400	0.97710	0.22030
Na1	4e	0.65790	0.98400	0.51320
Na2	4e	0.84020	0.98790	0.50240
P1	4e	0.21570	0.45130	0.39870
P2	4e	0.45720	0.56990	0.61070
P3	4e	0.88610	0.42970	0.39660
O1	4e	0.21660	0.76080	0.39560
O2	4e	0.46030	0.26210	0.63010
O3	4e	0.87860	0.73690	0.38320
O4	4e	0.08860	0.14680	0.03280
O5	4e	0.56650	0.84230	0.95800
O6	4e	0.76660	0.15780	0.03960
O7	4e	0.12400	0.32260	0.33160
O8	4e	0.74690	0.68170	0.68090
O9	4e	0.79740	0.28400	0.32930
O10	4e	0.41230	0.72580	0.67550
O11	4e	0.45250	0.29620	0.31010
O12	4e	0.06880	0.69830	0.67270

[1] G. Kresse and J. Furthmüller, Phys. Rev. B **54**, 11169 (1996).
[2] J. P. Perdew, K. Burke, and M. Ernzerhof, Phys. Rev. Lett. 77, 3865 (1996).
[3] F. Zhou, K. Kang, T. Maxisch, G. Ceder, and D. Morgan, Solid State Comm. **132**, 181 (2004).

Optimized bond lengths for $Na_{2/3}FePO_4$

Atom 1	Atom 2	Symmetry 2	Optimized Distances
Fe1	O8	1-x, 2-y, 1-z	2.2453
Fe1	O1	x, y, z	2.1482
Fe1	O11	0.5-x, 0.5+y, 0.5-z	2.0674
Fe1	O4	x, 1+y, z	2.0575
Fe1	O8	-0.5+x, 1.5-y, -0.5+z	2.0951
Fe1	O7	x, 1+y, z	2.3921
Fe2	O11	1-x, -y, 1-z	2.1787
Fe2	O7	0.5+x, 0.5-y, 0.5+z	2.0378
Fe2	O5	x, -1+y, z	1.9670
Fe2	O12	0.5-x, -0.5+y, 1.5-z	1.9986
Fe2	O10	x, -1+y, z	2.0996
Fe2	O2	x, y, z	2.0221
Fe3	O10	0.5+x, 1.5-y, -0.5+z	2.1830
Fe3	O12	1-x, 2-y, 1-z	2.3391
Fe3	O3	x, y, z	2.0522
Fe3	O9	x, 1+y, z	2.2084
Fe3	O6	x, 1+y, z	2.0618
Fe3	O9	1.5-x, 0.5+y, 0.5-z	2.1955
Na1	O10	1-x, 2-y, 1-z	2.4152
Na1	O6	1.5-x, 0.5+y, 0.5-z	2.4035
Na1	O4	0.5+x, 1.5-y, 0.5+z	2.2972
Na1	O1	1-x, 2-y, 1-z	2.3376
Na1	O8	x, y, z	2.3576
Na1	O2	1-x, 1-y, 1-z	2.2990
Na2	O6	1.5-x, 0.5+y, 0.5-z	2.3879
Na2	O9	x, 1+y, z	2.3198
Na2	O3	x, y, z	2.2537
Na2	O7	1-x, 1-y, 1-z	2.3225
Na2	O1	1-x, 2-y, 1-z	2.3221
Na2	O5	1.5-x, 0.5+y, 1.5-z	2.3146
P1	O1	x, y, z	1.5287
P1	O8	1-x, 1-y, 1-z	1.5705
P1	O6	-0.5+x, 0.5-y, 0.5+z	1.5471
P1	O7	x, y, z	1.5726
P2	O2	x, y, z	1.5339
P2	O4	0.5-x, 0.5+y, 0.5-z	1.5241
P2	O11	1-x, 1-y, 1-z	1.5660
P2	O10	x, y, z	1.5850
P3	O12	1-x, 1-y, 1-z	1.5683
P3	O3	x, y, z	1.5239
P3	O5	1.5-x, -0.5+y, 1.5-z	1.5562
P3	O9	x, y, z	1.5657

Geometry optimization for the olivine $Li_{2/3}FePO_4$

The electronic structure of the olivine $Li_{2/3}FePO_4$ was calculated with the VASP package[4] within the PBE[5] generalized gradient approximation (GGA). A GGA+U with (U_{eff}=4.3eV)[6] and a ferromagnetic order to better describe the correlation on the Fe d orbitals. Cell parameters were taken from experimental values while the atomic positions were optimized to minimize forces.

Details of the calculations:
Spin polarized calculation with a ferromagnetic coupling between Fe atoms
Energy Cut-Off for plane waves: 600eV
16 irreducible K-points for SCF (2, 8, 4) grid

Optimized structure of $Li_{2/3}FePO_4$:

Phase data

Space-group	P 1 21/n 1 (14) - monoclinic
Cell	a=17.8399 Å b=4.7552 Å c=11.8646 Å β=120.4850° V=867.36 Å^3

Atomic parameters

Atom	Wyck.	x/a	y/b	z/c
Fe1	4e	0.15706	0.96481	0.21937
Fe2	4e	0.50859	0.01611	0.78147
Fe3	4e	0.82262	0.96264	0.22306
Li1	4e	0.66485	0.00134	0.50088
Li2	4e	0.83909	0.98451	0.49869
P1	4e	0.21807	0.41935	0.40795
P2	4e	0.44966	0.58017	0.60068
P3	4e	0.88744	0.41356	0.40867
O1	4e	0.21901	0.74123	0.40510
O2	4e	0.45118	0.25980	0.61718
O3	4e	0.87945	0.73212	0.40114
O4	4e	0.09756	0.17623	0.04138
O5	4e	0.56564	0.80416	0.94788
O6	4e	0.76632	0.20538	0.04736
O7	4e	0.12324	0.29038	0.33755
O8	4e	0.74078	0.72236	0.66777
O9	4e	0.79645	0.26122	0.34002
O10	4e	0.40374	0.73565	0.66842
O11	4e	0.45787	0.28437	0.31766
O12	4e	0.06814	0.70829	0.66578

[4] G. Kresse and J. Furthmüller, Phys. Rev. B **54**, 11169 (1996).
[5] J. P. Perdew, K. Burke, and M. Ernzerhof, Phys. Rev. Lett. 77, 3865 (1996).
[6] F. Zhou, K. Kang, T. Maxisch, G. Ceder, and D. Morgan, Solid State Comm. **132**, 181 (2004).

Optimized bond lengths for $Li_{2/3}FePO_4$

Atom 1	Atom 2	Symmetry 2	Optimized Distances
Fe1	O8	1-x, 2-y, 1-z	2.2026
Fe1	O8	-0.5+x, 1.5-y, -0.5+z	2.0796
Fe1	O7	x, 1+y, z	2.3633
Fe1	O11	0.5-x, 0.5+y, 0.5-z	2.0541
Fe1	O1	x, y, z	2.1764
Fe1	O4	x, 1+y, z	2.0791
Fe2	O5	x, -1+y, z	1.9775
Fe2	O11	1-x, -y, 1-z	2.1207
Fe2	O7	0.5+x, 0.5-y, 0.5+z	2.0229
Fe2	O2	x, y, z	2.0411
Fe2	O10	x, -1+y, z	2.1285
Fe2	O12	0.5-x, -0.5+y, 1.5-z	1.9924
Fe3	O6	x, 1+y, z	2.1359
Fe3	O9	1.5-x, 0.5+y, 0.5-z	2.0921
Fe3	O9	x, 1+y, z	2.1947
Fe3	O3	x, y, z	2.1261
Fe3	O12	1-x, 2-y, 1-z	2.3191
Fe3	O10	0.5+x, 1.5-y, -0.5+z	2.0870
Li1	O6	1.5-x, -0.5+y, 0.5-z	2.1283
Li1	O10	1-x, 1-y, 1-z	2.1454
Li1	O4	0.5+x, 0.5-y, 0.5+z	2.1465
Li1	O2	1-x, -y, 1-z	2.2015
Li1	O1	1-x, 1-y, 1-z	2.1659
Li1	O8	x, -1+y, z	2.1895
Li2	O6	1.5-x, 0.5+y, 0.5-z	2.1340
Li2	O7	1-x, 1-y, 1-z	2.1472
Li2	O5	1.5-x, 0.5+y, 1.5-z	2.1231
Li2	O3	x, y, z	2.0357
Li2	O9	x, 1+y, z	2.0979
Li2	O1	1-x, 2-y, 1-z	2.2975
P1	O1	x, y, z	1.5312
P1	O6	-0.5+x, 0.5-y, 0.5+z	1.5440
P1	O8	1-x, 1-y, 1-z	1.5715
P1	O7	x, y, z	1.5818
P2	O11	1-x, 1-y, 1-z	1.5664
P2	O10	x, y, z	1.5910
P2	O4	0.5-x, 0.5+y, 0.5-z	1.5227
P2	O2	x, y, z	1.5345
P3	O5	1.5-x, -0.5+y, 1.5-z	1.5564
P3	O3	x, y, z	1.5199
P3	O9	x, y, z	1.5753
P3	O12	1-x, 1-y, 1-z	1.5667